

# Evidence for spontaneous breaking of a continuous symmetry at a non-conformal quantum critical point in one dimension

R. Flores-Calderón<sup>\*1,2</sup> and M. Zündel<sup>\*3</sup>

<sup>1</sup>Technical University of Munich, TUM School of Natural Sciences, Physics Department, 85748 Garching, Germany

<sup>2</sup>Munich Center for Quantum Science and Technology (MCQST), Schellingstr. 4, 80799 München, Germany

<sup>3</sup>Université Grenoble Alpes, CNRS, LPMMC, 38000 Grenoble, France

In this work, we present evidence for the spontaneous breaking of a continuous symmetry in a nearest-neighbour interacting spin-1 chain tuned to a quantum critical point at  $T = 0$  between two XY quasi-long-range order phases differing by the spontaneous breaking of a  $\mathbb{Z}_2$  symmetry. Despite the one-dimensional nature of the system, which typically prevents such a continuous symmetry breaking due to the Hohenberg-Mermin-Wagner theorem, the presence of a Berry phase term in the quantum model allows us to observe, using matrix product state methods, a finite perpendicular magnetization. Moreover, the quasi-long-range decay of the correlation function becomes truly long-range order, and the dynamical structure factor displays a characteristic Bragg peak together with sharp gapless modes. Our results imply the quantum phase transition has an anomalous dimension of  $\eta \simeq 1$  together with the dynamical critical exponent  $z \simeq 3/2$ , known from the Kardar-Parisi-Zhang universality class in one dimension. We perform a perturbative renormalization group calculation about the upper critical dimension  $d_c = 2$  that we could close at second loop order. We find an interacting fixed point with critical exponents distinct from the Ising ones. Together, our findings suggest the nature of the fixed point to be non-perturbative. We propose a field-theory that we believe to improve the quantitative results.

*Introduction.*— It is conventional wisdom that for spatial dimensions less than or equal to two, at finite temperature, the Hohenberg-Mermin-Wagner (HMW) theorem [1, 2] prevents spontaneous breaking of a continuous symmetry in a classical system. Over the years, various frameworks have emerged that relax certain assumptions of the HMW theorem, enabling continuous symmetry breaking in one dimension. They can be grouped into different physical mechanisms. The simplest example comes from the  $SO(3)$  symmetric Heisenberg ferromagnet [3–6]. Here, the breaking is allowed because the order parameter commutes with the Hamiltonian, and thus can be diagonalized simultaneously. The so-called frustration-free models of Ref. [7] generalized this example. Alternatively, it is known that long-range interactions can stabilize the spontaneous breaking of  $U(1)$  symmetry [8–11]. Finally, the possibility of breaking a continuous symmetry by escaping the constraints of thermal equilibrium has been demonstrated in non-equilibrium systems [12–15] and recently explored in open quantum systems [16, 17].

In this Letter, we present evidence for a continuous symmetry breaking at a quantum phase transition theorized recently by Nahum in Ref. [18]. The distinct physical mechanism that allows for the continuous symmetry breaking is the quantum nature of the spins, which gives rise to a topological Berry phase term. Such a term distinguishes our system from local classical models in 2D, allowing to circumvent the HMW theorem. We detect a quantum critical point at the transition between two XY quasi-long-range ordered (QLRO) phases differing by the spontaneous breaking of a  $\mathbb{Z}_2$  symmetry. We analyze the ground state of a spin-1 chain, with only local

nearest-neighbour exchange interactions. The field theory exhibiting this behaviour turns out to be a modification of the quantum Lifschitz model (QLM) [19–22]. The QLM is commonly studied in two spatial dimensions, where it describes the long-range physics of quantum dimer models in a quantum spin liquid phase [23–25].

In the following, we first present the model and the field theory we study, then we proceed to our numerical results using matrix product state (MPS) methods both for the static observables and for the dynamical spin structure factors. We calculate the critical exponents and present signatures of the XY LRO. Then, we set up a field theoretical renormalization group (RG) study to second order in  $\varepsilon$ . We find flow equations distinct from the Ising ones at second loop order and calculate the critical exponents at the interacting critical point. Finally, we suggest a model, we consider a starting point for non-perturbative calculations, to get a better quantitative result for the critical exponents at the fixed point. We conclude with a summary and discussion on future explorations.

*Model.*— Following the model proposed in Ref. [18] we will study the spin-1 Hamiltonian

$$H = \sum_{i=1}^L \left( -J \mathbf{S}_i \cdot \mathbf{S}_{i+1} + g_1 (S_i^z)^2 + g_2 (S_i^z S_{i+1}^z)^2 \right), \quad (1)$$

where  $\mathbf{S}_i$  are the spin-1 operators at site  $i$  of a periodic chain of length  $L$  and we will fix through this Letter the values  $J = 1$ ,  $g_2 = 1$ . The first term is a ferromagnetic Heisenberg exchange interaction; the second and last terms represent easy-plane single-ion and double-ion anisotropy, respectively. This model has several global symmetries. First, there is an  $O(2)$  symmetry implemented by rotating each spin around the  $z$  axis. Clearly, the Heisenberg term satisfies this symmetry. The remaining terms only have a  $z$ -component of the spin, thus are unchanged under the  $U(1)$  normal subgroup and can at most change by a sign belonging to the  $\mathbb{Z}_2$  subgroup in

<sup>\*</sup> Both authors contributed equally to this work  
r.flores-calderon@tum.de  
martina.zuendel@lpmmc.cnrs.fr

$O(2) = U(1) \rtimes \mathbb{Z}_2$ . It is the transition from a spontaneous symmetry-broken (SSB) phase to an unbroken state of the  $\mathbb{Z}_2$  subgroup that we will focus on in the following. Crucially, as we will see, the system on both sides of the transition is also in a quasi-long-range ordered (QLRO) XY phase. In the following section, we provide numerical evidence for an additional breaking of the  $U(1)$  symmetry at the  $\mathbb{Z}_2$  transition point. This is not a violation of the HMW theorem: As has been shown in [7], for a  $T = 0$  transition, the temperature in the Bogoliubov inequality gets replaced by the dispersion relation. Since our model is gapless with a large enough dynamical critical exponent, and additionally, there is no vanishing external magnetic field, the proof does not constrain the magnetization.

In the continuum limit, under the assumption of a small order parameter  $\psi$  close to the transition and keeping only RG-marginal and relevant terms, see Supplementary Material (SM), we map the partition function with the Hamiltonian of Eq. (1) to a theory with the following Euclidean Lagrangian (in imaginary time  $\tau$ )

$$\mathcal{L}_1 = i\psi\partial_\tau\theta + \frac{J}{2}[(\partial_x\psi)^2 + (\partial_x\theta)^2] + g_1\psi^2 + g_2\psi^4. \quad (2)$$

where  $\theta(x, \tau) \in [0, 2\pi)$  is the azimuthal angle field of the spin in the coherent state basis and  $\psi(x, \tau)$  is the field corresponding to the  $z$ -component of the spin. The first term in Eq. (8) is the Berry phase term, present in any spin system. The imaginary time is defined in the interval  $\tau \in (0, \beta]$ , with  $\beta = 1/T$ ,  $T$  the temperature, which we take to be zero in the following. The origin of this term relies on the quantization of the spin, here  $S = 1$ . The Berry phase term is of topological origin and allows the theory to differ from usual  $O(2)$  statistical models. Importantly, the coefficient of the term will not renormalize, and the RG equations will depend strongly on this. Additionally, the first term tells us that  $\theta$  and  $\psi$  are conjugate variables. Furthermore, the  $\theta$  field is gapless while the  $\psi$  field has a mass  $g_1$  and a  $\psi^4$  interaction parametrized by the coupling  $g_2$ .

*Static observables.*— We use the infinite density matrix renormalization group (iDMRG) algorithm [26, 27], performed with the TenPy library [28, 29], to first calculate the ground state of Eq. (1), and then, using the time-evolving block decimation (TEBD) algorithm [30–32] to evolve our state in time. In the SM, we give more details of the benchmarking and the method. Let us look first at the  $z$ -magnetization density in the ground state, defined as  $m_z = \frac{1}{L} \sum_i \langle S_i^z \rangle$ . We follow the entanglement-scaling analysis of critical points similar to Refs. [33–37]. We compute this for increasing bond dimension  $\chi$  as a function of the parameter  $g_1$  as shown in Fig. 1a. For parameter values  $g_1$  less than approximately  $-0.82$  we find  $m_z \neq 0$  consistent with a  $\mathbb{Z}_2$  SSB phase. Additionally, the magnetization has very similar values for different bond dimensions. In contrast, for  $g_1$  bigger than  $-0.82$  the magnetization has a very small value close to zero  $m_z$ , consistent with an unbroken  $\mathbb{Z}_2$  phase. We are interested in the value of the tuning parameter  $g_1$  for which the magnitude of the magnetization first goes to zero. The value of the coupling  $g_c$  can be deduced by performing a fit of the order

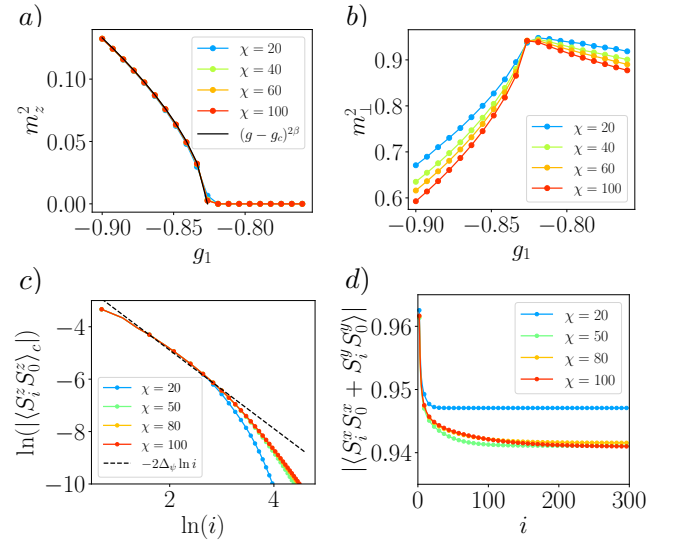


FIG. 1: a) Order parameter  $m_z^2$  vs coupling  $g_1$  calculated in the ground state of Eq. (1) using iDMRG. We vary the bond dimension  $\chi$  and perform a power-law fit at  $\chi = 100$ , finding a critical exponent of  $\beta = 0.30 \pm 0.01$  and the fixed point value  $g_c = -0.826 \pm 0.005$ . b) The perpendicular magnetization  $m_\perp$  shows a decreasing behaviour with increasing bond dimension, consistent with a QLRO of the XY type. Nevertheless, at the critical point of a) the magnetization stays approximately constant. It becomes a local maximum as a function of  $g_1$ . c) Log-log plot of the equal-time connected correlation function for the  $S_i^z$  component of the spin. We plot the correlations for different values of  $\chi$ , finding a linear regime, where we observe a collapse for different bond dimensions. Performing a fit at  $\chi = 100$ , we find the relation of Eq. (4). d) Plot of the XY correlation function as a function of position for  $g_1 = g_c$ . We observe that close to the critical point and at large distances, the correlator behaves like a constant, i.e. the XY component is LRO.

parameter  $m_z$  to a power-law. We find for the largest chosen bond dimension  $\chi = 100$  a value  $g_c = -0.826 \pm 0.005$ . The behavior of  $m_z$  is fitted to the critical exponent  $\beta$  by

$$m_z^2 \propto (g - g_c)^{2\beta}, \quad \beta = 0.30 \pm 0.01, \quad (3)$$

Further confirmation of the phase transition as a function of  $g_1$  comes from the connected correlation function of the  $z$ -component of the spin. We define this as  $\langle S_i^z S_0^z \rangle_c = \langle S_i^z S_0^z \rangle - \langle S_i^z \rangle \langle S_0^z \rangle$ . We plot the logarithm of the absolute value of this quantity at  $g_c$  vs  $\ln(i)$  for different bond dimensions  $\chi$  in Fig. 1c. Within the window of values, shown in the figure, we observe a linear dependence. This is consistent with the fact that for large distances we reached the correlation length and the correlator decays exponentially, while the short-distance physics is not universal. Indeed, in between the curves of different bond dimensions overlap and we deduce from the fit that

$$\langle S_x^z S_0^z \rangle_c \propto \frac{1}{|x|^{2\Delta_\psi}}, \quad \Delta_\psi = 0.75 \pm 0.03, \quad (4)$$

where we defined  $\Delta_\psi$  to be the scaling dimension of the  $S^z$  operator, which in the field theory becomes the  $\psi$  field. Note

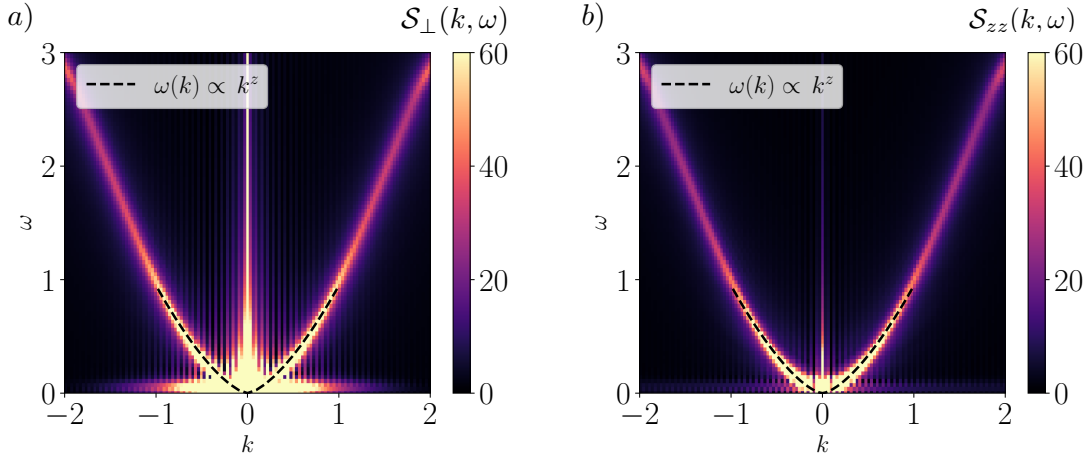


FIG. 2: Dynamical spin structure factor as a function of frequency and momentum for the a) perpendicular Eq. (6) and b) parallel spin components Eq. (5). For the simulations we use an MPS of bond dimension  $\chi = 100$  and extent  $L = 200$ , the time evolution is done for  $\Delta t = 0.1$  and 600 time steps. A Gaussian window function with  $\sigma = 0.2$  is applied to the time data. We extract the maxima of  $S_{zz}$  and perform a log-log fit of the data as a function of frequency and momentum for long-wavelengths, shown in the inset of b). We find the relation  $\omega \propto k^z$  with  $z = 1.51 \pm 0.03$ .

at this level that for a quantum phase transition, we expect the critical exponent to be given by  $\Delta_\psi = (d + z + \eta - 2)/2$ , with  $d = 1$  the spatial dimension,  $z$  the dynamical critical exponent, and  $\eta$  the anomalous dimension. The mean field exponents of Eq. (8) are given by  $z = 2, \eta = 0$ . We expect them to change as we renormalize the theory. Indeed, this will be shown in the 2-loop RG section. Here, we deduce the numerical relation  $z + \eta = 2.5 \pm 0.03$ .

To check for signs of LRO we calculate the perpendicular magnetization density in the ground state, defined as  $m_\perp = \frac{1}{L} \sum_i \langle S_i^x \rangle + \langle S_i^y \rangle$  and shown in Fig. 1b as a function of  $g_1$ . We observe that for both sides of the transition  $m_\perp \neq 0$ , but as the bond dimension is increased, the magnetization decreases. This indicates that for the true ground state, there is no true LRO and  $m_\perp \rightarrow 0$  in the thermodynamic limit, instead only QLRO survives. We further confirm this by plotting the entanglement entropy and the correlation length against the coupling  $g_1$  for different bond dimensions, see the SM. Nevertheless, it is also clear that for the special point  $g = g_c$  this reduction is not present. As the bond dimension is increased, the magnetization tends to a finite value, which is consistent with true LRO. We further confirm this by plotting the correlation function  $\langle S_i^x S_0^x + S_i^y S_0^y \rangle$  at the transition point, as seen in Fig. 1d. Indeed, we observe that the logarithmic decay characteristic of a QLRO phase plateaus for large distances and converges as a function of increasing bond dimension. We deduce that  $\langle S_i^x S_0^x + S_i^y S_0^y \rangle \rightarrow \langle S_i^x \rangle \langle S_0^x \rangle + \langle S_i^y \rangle \langle S_0^y \rangle \propto \langle S_i^x \rangle^2 + \langle S_i^y \rangle^2 \propto m_\perp^2$ . Indeed, there is a nice agreement between the plateau value of the correlations in Fig. 1d and the  $m_\perp$  at the critical point in Fig. 1b.

It is also worth noting that the order parameter  $m_z$  goes to zero at the same point that the XY order parameter  $m_\perp$  has a maximum. This is consistent with the intuition that the increased fluctuations of the  $z$ -component of the spin close to

the critical point imply reduced fluctuations for the perpendicular components due to the fixed spin-length constraint and the spin commutation relations.

*Dynamical structure factor.*— To obtain the complete set of critical exponents, and further confirm the XY LRO we must analyze the dynamics of the system. We do this by calculating two dynamical structure factors

$$S_{zz}(k, \omega) = \sum_j \int dt e^{i(\omega t - k j)} \langle S_j^z(t) S_0^z(0) \rangle, \quad (5)$$

$$S_\perp(k, \omega) = \sum_j \int dt e^{i(\omega t - k j)} \langle S_j^x(t) S_0^x(0) + S_j^y(t) S_0^y(0) \rangle. \quad (6)$$

The first quantity details the dynamics of the  $z$ -component of the spin, while the second of the perpendicular components, here we used the lattice spacing  $a = 1$ . We are interested in the universal regime of the low-frequency and long-wavelength limit. This regime will contain the critical properties of the quantum critical point. We plot the results at the critical point  $g_1 = g_c$  in Fig. 2 for a system of  $L = 200$  sites,  $\chi_{\max} = 100$  with 600 time-steps each with  $\Delta t = 0.1$ . We observe sharp modes in the spectrum of both  $S_{zz}$  and  $S_\perp$ . These modes come down in energy and touch the  $\omega = 0$  point at  $k = 0$ , consistent with a gapless critical point. The spectral weight has a very strong delta-like peak in  $S_\perp$  as seen in Fig. 2b, this peak is the Bragg peak consistent with  $U(1)$  SSB. We further analyze the critical properties of the dynamical structure factor by extracting the maxima of the  $S_{zz}(k, \omega)$  spectral values for small  $k$  and fitting the data to a power-law  $\omega \propto k^z$ , as seen in the inset of Fig. 2b. The result is a dynamical critical exponent of

$$z = 1.51 \pm 0.03, \quad \eta = 1.01 \pm 0.03, \quad (7)$$

where the previous numerical relation determines the anomalous dimension. We explain details on the fits and error estimates in the SM. Remarkably, the numerical value of the anomalous dimension, together with the dynamical critical exponent, is consistent with the first renormalization condition found in the effective field theory. Note in particular that the approximate value of  $z$  is also found for the perpendicular dynamical structure factor. A further validation of the exponent  $\eta$  was obtained by fitting the correlator in momentum-space  $S_{zz}(k, \omega = 0)$ , which is expected to scale as  $k^{-2+\eta}$ . The resulting value agrees well with that extracted from the static correlators, as shown in the SM. We proceed to study the criticality of the Lagrangian (8) from a perturbative renormalization group approach.

*Dimensional regularization and Ward identities.*— We perform a perturbative renormalization and a simultaneous expansion about the upper critical dimension  $d_c = 2$ . To simplify the calculation, we start from the massless Lagrangian

$$\mathcal{L}[\theta, \psi] = i\psi \partial_\tau \theta + \frac{K}{2} (\nabla \theta)^2 + \frac{1}{2} (\nabla \psi)^2 + \frac{g}{4!} \psi^4, \quad (8)$$

and introduce the mass as a perturbation in a second step. We introduce in the following the renormalized Lagrangian  $\mathcal{L}_R$  by multiplicative renormalization. The bare couplings are related by renormalization constants  $Z$  to the renormalized couplings, indicated with an index  $R$ :

$$\theta = Z_\theta^{1/2} \theta_R, \quad \psi = Z_\psi^{1/2} \psi_R, \quad K = \frac{Z_K}{Z_\theta} K_R, \quad g = \frac{\mu^\varepsilon Z_g}{Z_\psi^2} g_R, \quad (9)$$

where the scale  $\mu$  is the renormalization scale,  $g_R$  is a dimensionless coupling. The effective action  $\Gamma_R$ , generator of the one-particle irreducible correlation functions, is given by the Legendre transformation  $\Gamma[\phi] = J_a \phi_a - W[J]$  of the Schwinger functional  $e^{W[J]} = \int \mathcal{D}[\varphi] e^{-S[\varphi] + J_a \varphi_a}$ , here field  $\varphi$ , mean field  $\phi$  and sources  $J$  have two components:  $\psi$  and  $\theta$ . We use de Witt notation and Einstein's sum convention. We abbreviate functional derivatives as  $S^{\varphi_1 \dots \varphi_n} = \frac{\delta^n}{\delta \varphi_1 \dots \delta \varphi_n} S$ .

We deduce two renormalization conditions constraining the  $Z$ -factors: First, the non-renormalizability of the Berry phase term  $\partial_\omega \Gamma_R^{\psi\theta}|_{\text{NP}} = 1$  leading to  $Z_\psi = Z_\theta^{-1} \equiv Z$ , meaning the conjugate fields  $\theta_R$  and  $\psi_R$  are renormalized by one constant only. Second,  $\Gamma_R^{\theta\theta} = S^{\theta\theta}$  leading to  $Z_K K_R = K$ . This Ward identity is equivalent to the observation that the self-energy  $\Sigma^{\theta\theta} = 0$  is identical to zero to all loop orders since there are no bare vertices that have  $\theta$ -legs. In the SM, we explain how the Ward identities can be derived from the infinitesimal shift  $\theta(x, t) \mapsto \theta(x, t) + \epsilon(x, t)$ . The regularized Lagrangian therefore, reads

$$\mathcal{L}_R = i\psi_R \partial_\tau \theta_R + \frac{K}{2} (\nabla \theta_R)^2 + \frac{1}{2} Z (\nabla \psi_R)^2 + \frac{g_R}{4!} \mu^\varepsilon Z_g \psi_R^4. \quad (10)$$

Astonishingly, the number of running couplings corresponds exactly to the textbook [38] massless  $\phi^4$ -theory. Since we are interested in the behaviour of the correlation functions near criticality by tuning the relevant parameter, i.e. the mass, we

add a source term for the monomial  $\psi_R^2$  to the action. We write

$$\mathcal{L}_R[\theta_R, \psi_R, \psi_R^2] = \mathcal{L}_R[\theta_R, \psi_R] + \frac{1}{2} m_R^2 Z_2 \psi_R^2, \quad (11)$$

where with respect to the initial action  $m^2 = m_R^2 Z_2 Z^{-1}$ . In the SM, we detail how to carry out the calculation in dimension  $d = 2 - \varepsilon$  in the minimal subtraction  $\overline{MS}$  scheme. In the following, we use an effective coupling, absorbing the loop factors  $\tilde{g} := \frac{\sqrt{K}}{8\pi} g_R$ .

At one-loop order, the flow equations are equivalent to the Ising ones, where the expansion is done around the upper critical dimension  $d_c^{(\text{Ising})} = 4$ , instead of  $d_c = 2$ . Therefore, the critical exponents also correspond to the Ising universality class, in agreement with Ref. [18].

*Two-loop results.*— In a very similar way to the two-loop calculation for the Ising model [38], we calculate the corrections to two-loop order; all details are given in the SM. We give here only the resulting flow equations, which differ from the Ising ones

$$\tilde{\beta}(\tilde{g}) = -\varepsilon \tilde{g} + \frac{3}{2} \tilde{g}^2 + \gamma_1 \tilde{g}^3 + \mathcal{O}(\tilde{g}^4), \quad (12)$$

$$\eta(\tilde{g}) = \frac{1}{27} \tilde{g}^2 + \mathcal{O}(\tilde{g}^3), \quad (13)$$

$$\eta_2(\tilde{g}) = -\frac{\tilde{g}}{2} + \gamma_2 \tilde{g}^2 + \mathcal{O}(\tilde{g}^3), \quad (14)$$

with  $\gamma_1 := \frac{2}{27} + \frac{1}{4} + 3 \ln 2 - \frac{3}{2} \ln 3$  and  $\gamma_2 := -\frac{1}{2} \ln 2 + \frac{1}{4} \ln 3 - \frac{1}{24} - \frac{1}{27}$ . The positive, non-zero fixed point solution is given to second order in epsilon by  $\tilde{g}^* = \frac{2}{3} \varepsilon - \frac{8}{27} \gamma_1 \varepsilon^2 + \mathcal{O}(\varepsilon^3)$ . We obtain the critical exponents  $\eta = \frac{4}{243} \varepsilon^2$ , hence  $z = 2 - \frac{2}{243} \varepsilon^2$  and  $2\nu = 1 + \frac{1}{6} \varepsilon - [\frac{1}{36} + \frac{2}{9} \gamma_2 + \frac{2}{27} \gamma_1] \varepsilon^2$ .

*Non-perturbative fixed point.*— The results obtained from the perturbative renormalization differ from the numerical prediction: The corrections to the bare exponents are large, whereas the RG predicts only small deviations. This indicates either slow convergence or the failure of a perturbative approach, which is based on the proximity to the Gaussian fixed point due to the bare power counting. This leads us to the hypothesis, that the nature of the fixed point might be non-perturbative. Then, the action (8) based on the relevance of the operators is not a good quantitative starting point to predict the critical exponents. We propose, based on the derivation in the SM, a Landau-Ginzburg type of Lagrangian having additional terms, for clarity given in terms of the original Hamiltonian (1) couplings,

$$\mathcal{L}_1 + (\frac{J}{2} - 2g_2) \psi^2 (\partial_x \psi)^2 - \frac{J}{2} \psi^2 (\partial_x \theta)^2. \quad (15)$$

It displays less trivial dynamics: Even though the Lagrangian is still quadratic in  $\theta$ , there are now bare vertices containing  $\theta$ , such that the second Ward identity no longer holds.

*Discussion and outlook.*— In this work, we investigated the quantum phase transition in a spin-1 chain between two QLRO XY phases distinguished by a nonzero  $\mathbb{Z}_2$  order parameter, combining analytical and MPS numerical methods.

Our results show that the transition described by Eq. (1) is continuous, with order parameter  $m_z$ . At criticality, we observe signatures of XY long-range order: a finite perpendicular magnetization  $m_\perp$ , non-decaying XY correlations, and a zero-frequency, zero-momentum Bragg peak in the perpendicular dynamical structure factor, indicating Bose condensation. Sharp gapless excitations appear in both longitudinal and transverse channels. The presence of sharp gapless modes in a strongly-interacting  $T = 0$  equilibrium theory in one spatial dimension is remarkable. Specifically, we note that the SSB of the discrete  $\mathbb{Z}_2$  symmetry cannot lead to Goldstone modes, and in one dimension, gapless modes are typically part of a continuum, as is well-known for the antiferromagnetic Heisenberg model. We determine the critical exponents characterizing the universality class of this transition, finding  $\eta = 1.01 \pm 0.03$ , a dynamical exponent  $z = 1.51 \pm 0.03$ , and  $\beta = 0.30 \pm 0.01$ , consistent with the constraints imposed by the field theory in Eq. (8). It is fascinating that the dynamical critical exponent matches the one-dimensional KPZ critical exponent  $z = 3/2$  well. The KPZ universality class governs the scaling and statistics of countless non-equilibrium phenomena in nature, and it was also found in quenched quantum spin chains [39–42]. However, to the best of our knowledge, this is the first time  $z \simeq 3/2$  was found in a quantum system at equilibrium: It is striking, especially, since the KPZ equation itself is a stochastic evolution equation that is out-of-equilibrium. Only in one dimension, it fulfills a time-reversal symmetry. Therefore, it seems crucial to reach a deeper understanding of the correct effective description and symmetries governing the fixed point behavior. Also, it would be interesting to further analyze the phase diagram of the model as a function of  $g_1, g_2$ , and to explore if a spin-1/2 model can realize this physics. Experimental platforms, such as Rydberg atoms [43, 44], a quantum gas microscope [45] and possibly magnons [46], could realize the model and probe the exciting features of the phase diagram.

Complementary to the numerical study, we performed a perturbative RG calculation using dimensional regularization. We derived the complete set of flow equations to second order in the coupling which differ from the Ising model. Also, the critical exponents at the interacting fixed point differ from the Ising universality class at second order in  $\varepsilon$ . We obtain a finite anomalous dimension  $\eta$  and a dynamical critical exponent  $z$  deviating from the bare value, in contrast to the one-loop result of Ref. [18]. However, these corrections are small, suggesting that a non-perturbative study is required to quantitatively describe this transition and determine its universality class.

**Acknowledgements.**— We gratefully acknowledge fruitful discussions with M. Heinrich, A. Al-Eryani, L. Gosteva, M. Buchhold, S. Ray and F. Pollmann. MZ thanks RF for bringing up Ref. [18]. This research was undertaken in part at the Max Planck Institute for the Physics of Complex Systems in Dresden, Germany.

- 
- [1] P. C. Hohenberg, *Physical Review* **158**, 383 (1967).
  - [2] N. D. Mermin and H. Wagner, *Physical Review Letters* **17**, 1133 (1966).
  - [3] P. W. Anderson, *Basic Notions of Condensed Matter Physics* (CRC Press, Boca Raton, Florida, 2018).
  - [4] M. B. Zvonarev, V. V. Cheianov, and T. Giamarchi, *Physical Review Letters* **99**, 240404 (2007).
  - [5] A. J. Beekman, L. Rademaker, and J. van Wezel, *SciPost Physics Lecture Notes* **10.21468/SciPostPhysLectNotes.11** (2019).
  - [6] H. Watanabe, *Annual Review of Condensed Matter Physics* **11**, 169 (2020).
  - [7] H. Watanabe, H. Katsura, and J. Y. Lee, *Phys. Rev. Lett.* **133**, 176001 (2024).
  - [8] M. F. Maghrebi, Z.-X. Gong, and A. V. Gorshkov, *Physical Review Letters* **119**, 023001 (2017).
  - [9] Z.-X. Gong, M. F. Maghrebi, A. Hu, M. Foss-Feig, P. Richerme, C. Monroe, and A. V. Gorshkov, *Phys. Rev. B* **93**, 205115 (2016).
  - [10] A. Romen, S. Birnkammer, and M. Knap, *SciPost Phys. Core* **7**, 008 (2024).
  - [11] L. Feng, O. Katz, C. Haack, M. Maghrebi, A. V. Gorshkov, Z. Gong, M. Cetina, and C. Monroe, *Nature* **623**, 713 (2023).
  - [12] T. Vicsek, A. Czirók, E. Ben-Jacob, I. Cohen, and O. Shochet, *Phys. Rev. Lett.* **75**, 1226 (1995).
  - [13] J. Toner and Y. Tu, *Phys. Rev. Lett.* **75**, 4326 (1995).
  - [14] K. E. Bassler and Z. Rácz, *Phys. Rev. E* **52**, R9 (1995).
  - [15] F. Corberi, G. Gonnella, E. Lippiello, and M. Zannetti, *Journal of Physics A: Mathematical and General* **36**, 4729–4755 (2003).
  - [16] P. Sala, *Physical Review B* **110**, 155150 (2024).
  - [17] T. Orito, Y. Kuno, and I. Ichinose, *Physical Review B* **10.1103/PhysRevB.111.045112** (2025), in press.
  - [18] A. Nahum, *Continuous symmetry breaking in 1d spin chains and 1+1d field theory* (2025), [arXiv:2506.21540 \[cond-mat.stat-mech\]](https://arxiv.org/abs/2506.21540).
  - [19] C. Bervillier, *Physics Letters A* **331**, 110 (2004).
  - [20] G. Grinstein, *Physical Review B* **23**, 4615 (1981).
  - [21] E. Fradkin, D. A. Huse, R. Moessner, V. Oganesyan, and S. L. Sondhi, *Physical Review B* **69**, 224415 (2004).
  - [22] B. Hsu and E. Fradkin, *Physical Review B* **87**, 085102 (2013).
  - [23] D. S. Rokhsar and S. A. Kivelson, *Physical Review Letters* **61**, 2376 (1988).
  - [24] E. Ardonne, P. Fendley, and E. Fradkin, *Annals of Physics* **310**, 493 (2004).
  - [25] S. V. Isakov, M. B. Hastings, S. Trebst, R. G. Melko, and R. Moessner, *Physical Review B* **83**, 125114 (2011).
  - [26] S. R. White, *Physical Review Letters* **69**, 2863 (1992).
  - [27] S. R. White, *Phys. Rev. B* **48**, 10345 (1993).
  - [28] J. Hauschild, J. Unfried, S. Anand, B. Andrews, M. Bintz, U. Borla, S. Divic, M. Drescher, J. Geiger, M. Hefel, K. Hémerly, W. Kadow, J. Kemp, N. Kirchner, V. S. Liu, G. Möller, D. Parker, M. Rader, A. Romen, S. Scalet, L. Schoonderwoerd, M. Schulz, T. Soejima, P. Thoma, Y. Wu, P. Zechmann, L. Zweng, R. S. K. Mong, M. P. Zaletel, and F. Pollmann, *SciPost Phys. Codebases*, 41 (2024).
  - [29] J. Hauschild and F. Pollmann, *SciPost Phys. Lect. Notes*, 5 (2018).
  - [30] G. Vidal, *Phys. Rev. Lett.* **91**, 147902 (2003).
  - [31] G. Vidal, *Physical Review Letters* **93**, 040502 (2004).
  - [32] S. R. White and A. E. Feiguin, *Physical Review Letters* **93**, 076401 (2004).

- [33] M. B. Hastings, *Journal of Statistical Mechanics: Theory and Experiment* **2007**, P08024 (2007).
- [34] G. Vidal, *Physical Review Letters* **101**, 110501 (2008).
- [35] L., T. R. de Oliveira, S. Iblisdir, and J. I. Latorre, *Phys. Rev. B* **78**, 024410 (2008).
- [36] J. C. Pillay and I. P. McCulloch, *Phys. Rev. B* **100**, 235140 (2019).
- [37] V. Stojevic, J. Haegeman, I. P. McCulloch, L. Tagliacozzo, and F. Verstraete, *Physical Review B* **91**, 035120 (2015), arXiv:1401.7654 [quant-ph].
- [38] J. Zinn-Justin, *Quantum field theory and critical phenomena*, 5th ed., International Series of Monographs on Physics (Oxford University Press, London, England, 2021).
- [39] M. Ljubotina, M. Žnidarič, and T. Prosen, *Physical Review Letters* **122**, 210602 (2019).
- [40] D. Wei, A. Rubio-Abadal, B. Ye, F. Machado, J. Kemp, K. Srakaew, S. Hollerith, J. Rui, S. Gopalakrishnan, N. Y. Yao, I. Bloch, and J. Zeiher, *Science* **376**, 716–720 (2022).
- [41] B. Ye, F. Heidrich-Meisner, and E. Ilievski, *Physical Review Letters* **129**, 230602 (2022).
- [42] E. Rosenberg, T. I. Andersen, R. Samajdar, A. Petukhov, J. C. Hoke, D. Abanin, A. Bengtsson, I. K. Drozdov, C. Erickson, P. V. Klimov, X. Mi, A. Morvan, M. Neeley, C. Neill, R. Acharya, R. Allen, K. Anderson, M. Ansmann, and F. . Arute, *Science* **384**, 48–53 (2024).
- [43] P. Sompet, S. Hirthe, D. Bourgund, T. Chalopin, J. Bibo, J. Koepsell, P. Bojović, R. Verresen, F. Pollmann, G. Salomon, C. Gross, T. A. Hilker, and I. Bloch, *Nature* **606**, 484–488 (2022).
- [44] A. Luo, Y.-G. Zheng, W.-Y. Zhang, M.-G. He, Y.-C. Shen, Z.-H. Zhu, Z.-S. Yuan, and J.-W. Pan, *Phys. Rev. Lett.* **133**, 043401 (2024).
- [45] J. Mögerle, K. Brechtelsbauer, A. Gea-Caballero, J. Prior, G. Emperauger, G. Bornet, C. Chen, T. Lahaye, A. Browaeys, and H. Büchler, *PRX Quantum* **6**, 020332 (2025).
- [46] P. Chauhan, F. Mahmood, H. J. Changlani, S. M. Koohpayeh, and N. P. Armitage, *Phys. Rev. Lett.* **124**, 037203 (2020).
- [47] I. S. Gradshteyn and I. M. Ryzhik, *Table of Integrals, Series, and Products*, 8th ed., edited by D. Zwillinger and V. H. Moll (Academic Press / Elsevier, Amsterdam, 2015).

# Supplemental material for “Evidence for spontaneous breaking of a continuous symmetry at a non-conformal quantum critical point”

R. Flores-Calderón,<sup>1,2</sup> M. Zündel,<sup>3</sup>

<sup>1</sup>Technical University of Munich, TUM School of Natural Sciences, Physics Department, 85748 Garching, Germany

<sup>2</sup>Munich Center for Quantum Science and Technology (MCQST), Schellingstr. 4, 80799 München, Germany

<sup>3</sup>Université Grenoble Alpes, CNRS, LPMMC, 38000 Grenoble, France

## S1. Details on the numerical simulations

As mentioned in the main text, we employ MPS methods to study the ground state and dynamical properties of the spin-1 model Eq. (1). The ground state wavefunction was found using both iDMRG and finite DMRG. For the time evolution, we take the iDMRG ground state and repeat it several times in order to have a system size of  $L$ . We perform the additional sweeps using finite DMRG. As a last step we perform the time evolution using TEBD. We use a Gaussian kernel for the final Fourier transform with the form  $e^{-\sigma^2 t^2}$  and we use  $\sigma = 0.2$ . A check was done to ensure the entropy built by perturbing the ground state with  $S_0^\pm$  or  $S_0^z$  and time evolving does not hit the boundary of the system, as shown in Fig. S3.

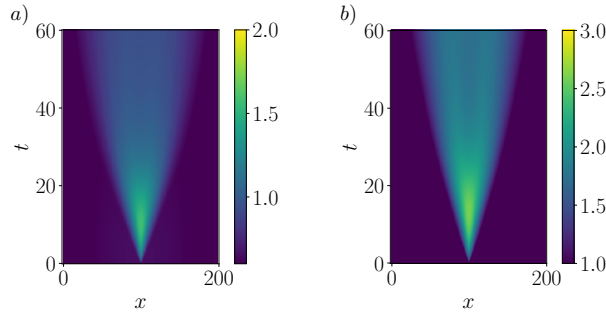


FIG. S3: Entanglement entropy as a function of time and space for the time evolution of the wave function used to calculate the main text dynamical structure factors a)  $S_\perp(k, \omega)$  and b)  $S_{zz}(k, \omega)$ . We use the critical coupling  $g_1 = g_c$ ,  $g_2 = J = 1$  and  $\Delta t = 0.1$ ,  $\chi = 100$ ,  $L = 200$  and  $T_{\max} = 60$ .

We computed static quantities with a slow increase in the bond dimension. After sufficiently many sweeps have been performed at a given low bond dimension, ensuring stability, we save the final wavefunction and use it as an initial guess for the next bond dimension. Furthermore, we use the wavefunction at the largest bond dimension for a fixed parameter value  $g_1$  as an initial guess for the next parameter  $g_1^* = g_1 + \delta g_1$ , with  $\delta g_1 = 0.007$ .

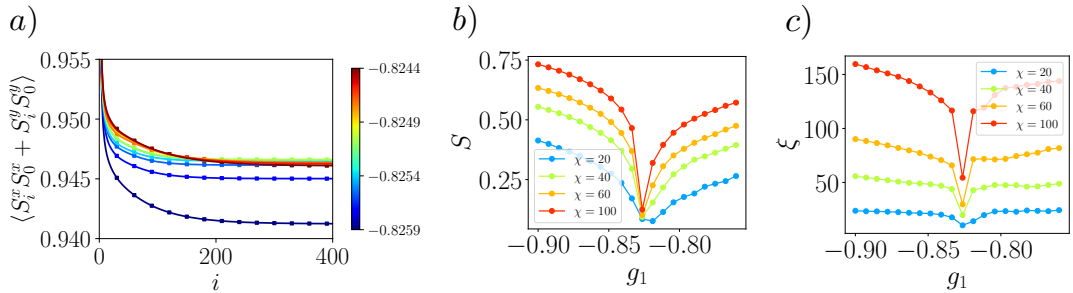


FIG. S4: iDMRG results for different bond dimension  $\chi$  of the model in the main text with  $g_2 = 1$ ,  $J = 1$ . We plot in a) the the XY correlation function as a function of the number of sites for  $g_1$  close to the critical point. b) Entanglement entropy as a function of coupling  $g_1$ . c) Correlation length as a function of coupling  $g_1$ .

In Fig. S4, we use this procedure to calculate the XY correlations at the quantum critical point as well as the entanglement entropy and the correlation length as a function of  $g_1$ . We observe that the correlation function for large distances stabilizes to a finite value; additionally as we tune to the critical point the power-law decay gets corrected to a plateau. The entanglement entropy in Fig. S4b increases as the bond dimension is increased at both sides of the transition. This behaviour is consistent with QLRO of the XY components of the spin. Such critical correlations imply a diverging correlation length, as is shown in

Fig. S4c. The special point  $g_1 = g_c$  displays the slowest increase in entropy and correlation length consistent with XY LRO and critical  $S^z$ .

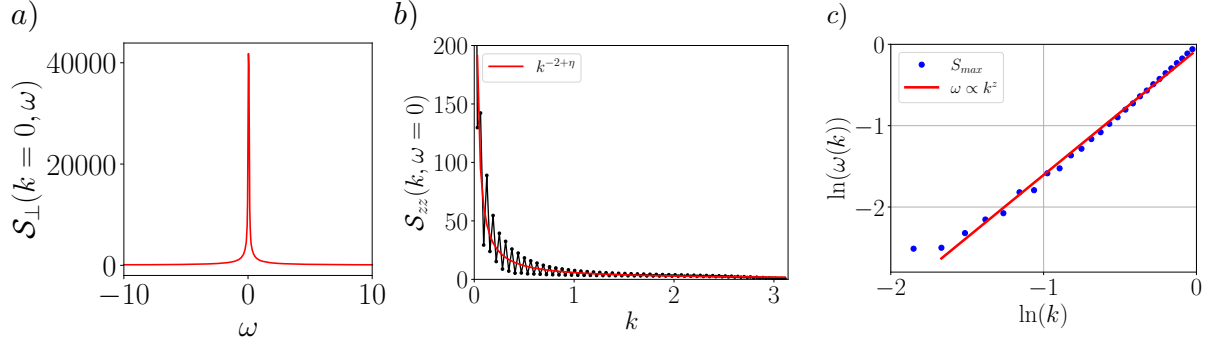


FIG. S5: Dynamical structure factor cuts for the main text plot showcasing a) Bragg peak or condensed fraction shown in  $S_{\perp}(k=0, \omega)$ . b) Longitudinal dynamical structure factor as a function of momentum  $S_{\perp}(k, \omega=0)$ , fit to a power-law  $\eta = 1.01 \pm 0.05$  consistent with the static results of the main text. c) Power-law fit with slope  $z = 1.51 \pm 0.03$ . Here we use the centers of a family of Gaussians fitted to each cut of the longitudinal spin structure factor at fixed momentum ranging from zero to one.

Further signatures of the order are presented in Fig S5a. We show the Bragg peak of the perpendicular component of the dynamical structure factor at zero momentum. The delta-like peak  $S_{\perp}(k, \omega) = L^2 \delta(k) \delta(\omega)$  indicates a bosonic condensate with a spontaneously broken  $U(1)$  symmetry. Furthermore we present fits for the critical exponents in Fig S5b,c. We estimate the error of the critical exponents, by performing a power-law fit to the data. We emphasize other errors from the bond dimension, system size, and time evolution are not considered. We do this for several intervals of points, recording the fit value and error. We then average over the values and estimate the total error from the variance of the values and the fit error. In Fig S5b we calculate the critical exponent  $\eta$  from the scaling relation  $S_{zz}(k, \omega=0) = \frac{1}{k^{2-\eta}}$  finding  $\eta = 1.01 \pm 0.05$  consistent with the static data of the main text. For the dynamical critical exponent  $z$  we first take cuts of  $S_{zz}(k, \omega)$  for fix  $k \in (0, 1)$  as a function of frequency. We then fit the functions to Gaussians in order to calculate the maximum of  $S_{\max}(k)$ . We plot this points in Fig S5c where we additionally perform the interval error analysis with intervals of points inside  $(\epsilon, 1)$  and  $\epsilon > 0$ . The values of the exponent were concentrated near 1.5 with a range from 1.48 for small  $\epsilon$  to 1.56 for larger  $\epsilon$  and had error fits of approximately 0.02 from which we extracted the value  $z = 1.51 \pm 0.03$ .

## S2. Data for $g_2 = 0.5$ and entanglement scaling

We additionally verify that the transition happens also for other values of  $g_2$  apart from the main text value  $g_2 = 1$ . We present our findings in Fig. S6 for  $g_2 = 0.5$ . We compute the perpendicular magnetization density  $m_z^2$  as a function of  $g_1$  in Fig. S6a. We find in this case that a transition also happens and find good convergence of  $m_z^2$  as a function of the bond dimension  $\chi$ . Moreover, we calculate the critical exponent  $\beta$  for this set of parameters from a fit of the  $m_z$  data to the functional form  $(g_1 - g_c)^\beta$ . We obtain for the largest bond dimension  $\chi = 100$  that the critical coupling is  $g_1 = -0.45 \pm 0.001$  and an exponent  $\beta = 0.31 \pm 0.01$ . It is worth commenting we find that the transition in the longitudinal component happens simultaneously with a maximum of the perpendicular magnetization  $m_{\perp}$  for fixed bond dimension as shown in Fig. S6b. We plot the entanglement entropy and correlation length in Fig. S6c and d. The divergence of the latter together with the fact that  $m_{\perp}$  decreases at both sides of the transition with increasing bond dimension indicates that the system is in an XY QLRO phase. At the transition the decrease of  $m_{\perp}$  is the slowest, consistent with true XY LRO.

Additionally, we calculate fits of the entanglement entropy as a function of the bond dimension in the QLRO phase as well as in our  $g_1 = g_c$  quantum phase transition. The results are shown in Fig. S7. In panel a) and c) we show the QLRO phase at the left and right of the transition point respectively. We find a consistent logarithmic scaling. The fit determines  $S = \kappa \ln \chi$  with  $\kappa = 0.2$ . This result is the expected scaling for a quantum critical point that is described by a conformal field theory (CFT), as was shown in Refs. [33–37]. In contrast, we show in Fig. S7b that the entanglement scaling does not follow such a scaling law together with the fact that  $z \approx 3/2$  we conclude that this is a non-CFT quantum critical point.

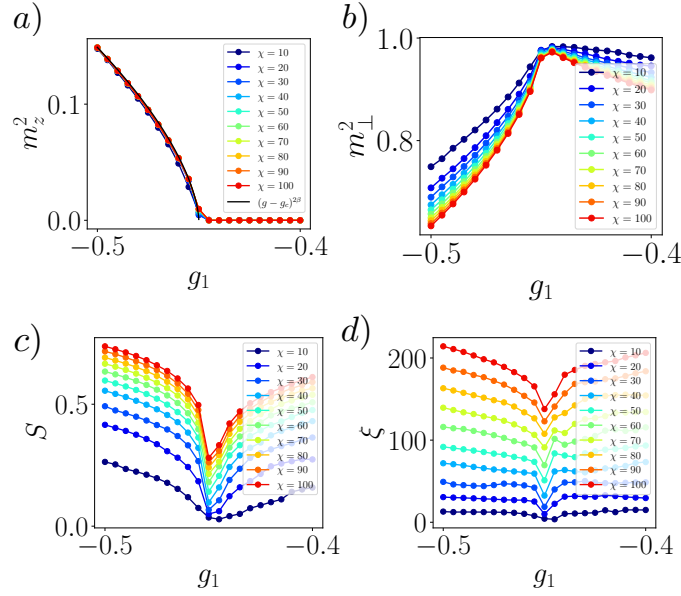


FIG. S6: Numerical results using iDMRG for the main text Hamiltonian with  $g_2 = 0.5$ ,  $J = 1$ , also showcasing a phase transition. We plot a) the square of the order parameter  $m_z$  for different bond dimension  $\chi$  and fit to a power-law giving  $\beta = 0.31 \pm 0.01$ , where the critical point is in this case  $g_c = -0.45 \pm 0.001$ . b) Perpendicular magnetization density for the same parameter values. We additionally plot the c) entanglement entropy and d) correlation length.

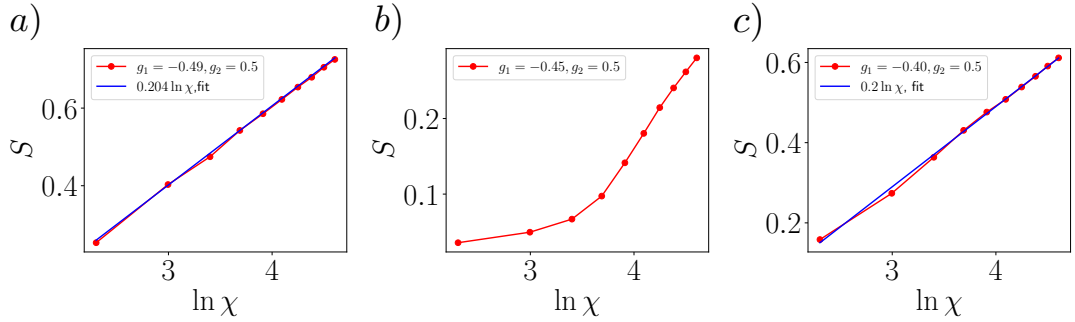


FIG. S7: Entanglement entropy scaling as a function of bond dimension for couplings  $g_2 = 0.5$ ,  $J = 1$ . We plot a) the scaling at the XY QLRO and Z LRO point  $g_1 = -0.49$ . We find a good fit to a logarithmic dependence, coefficient  $\kappa = 0.2$ , consistent with a conformal field theory (CFT) scaling. b) Non-logarithmic scaling at the  $g_1 = g_c = -0.45$  critical coupling, consistent with  $z \neq 1$ . c) Scaling at the XY QLRO and Z disorder point  $g_1 = -0.4$ . Fit reveals a similar logarithmic dependence  $\kappa = 0.201$  to a).

### S3. Derivation of the action

In this section, we derive the action starting from the Hamiltonian of Eq. (1). We use the coherent state representation of the spin, defined by the equation  $\langle \mathbf{n} | \mathbf{S} | \mathbf{n} \rangle = S \mathbf{n}$ , they form a basis  $1 = \frac{2S+1}{4\pi} \int d\Omega |\mathbf{n}\rangle \langle \mathbf{n}|$  and non-linear constraint  $\mathbf{n}^2 = 1$  must be satisfied at all times and for all sites. We parametrize the components of the vector such that the constraint is always satisfied by  $\mathbf{n} = (\sqrt{1-\psi^2} \cos \theta, \sqrt{1-\psi^2} \sin \theta, \psi)$  with  $\psi \in [-1, 1]$  and  $\theta \in (0, 2\pi]$ . Let us calculate the partition function of the quantum system by inserting identity operators at each discretized imaginary-time step. The usual procedure leads to the lattice action

$$S = \int_0^\beta d\tau \sum_{j=1}^N (-iS(1-\psi_j)) \partial_\tau \theta_j - JS^2 \mathbf{n}_j(\tau) \cdot \mathbf{n}_{j+1}(\tau) + g_1 (S n_j^z(\tau))^2 + g_2 (S n_j^z(\tau) S n_{j+1}^z(\tau))^2, \quad (\text{S1})$$

where we defined  $\mathbf{n}_j(\tau) = \mathbf{n}(x_j, \tau)$  the spin configuration at position  $x_j = aj$  and  $\Delta x_j = a$  is the lattice constant, we take  $N$  lattice sites. The first term comes from computing overlaps of coherent states at different times and is known as a Berry phase. The Berry phase ensures that  $S$  is a half-integer generically, in our case  $S = 1$  and we fix it in the following. We now want a

theory in the continuum  $a \rightarrow 0$  and  $N \rightarrow \infty$  while keeping  $Na = L$ . For this we perform an expansion in the lattice constant  $a$ . We expect this to be a good approximation near a second order phase transition where the correlation length is much larger than any lattice spacing. We express then  $\mathbf{n}_{j+1}(\tau) = \mathbf{n}(x_j, \tau) + a\partial_x \mathbf{n}(x_j, \tau) + \frac{a^2}{2}\partial_x^2 \mathbf{n}(x_j) + O(a^3)$ . We must enforce  $\mathbf{n}(x, \tau)^2 = 1$  at each space-time point. Furthermore, this implies  $\partial_x \mathbf{n} \cdot \mathbf{n} = 0$ . We use this to write

$$S = \int_0^\beta d\tau a^{-1} \int_0^L dx (-i(1 - \psi))\partial_\tau \theta - J\mathbf{n} \cdot (\mathbf{n} + \frac{a^2}{2}\partial_x^2 \mathbf{n}) + g_1 \psi^2 + g_2 \psi^2 (\psi + a\partial_x \psi + \frac{a^2}{2}\partial_x^2 \psi)^2 + O(a^3), \quad (S2)$$

where we also expanded the last terms. Now we use the expression

$$\partial_x \mathbf{n} = \left( \frac{\psi}{\sqrt{1 - \psi^2}} \partial_x \psi \cos \theta - \sqrt{1 - \psi^2} \sin \theta \partial_x \theta, \frac{\psi \partial_x \psi}{\sqrt{1 - \psi^2}} \sin \theta + \sqrt{1 - \psi^2} \cos \theta \partial_x \theta, \partial_x \psi \right). \quad (S3)$$

Integrating by parts we obtain

$$S = \int_0^\beta d\tau a^{-1} \int_0^L dx (-i(1 - \psi))\partial_\tau \theta - J + \frac{J}{2} a^2 (\partial_x \mathbf{n})^2 + g_1 \psi^2 + g_2 \psi^2 (\psi^2 + 2a\psi \partial_x \psi + a^2 (\partial_x \psi)^2 + a^2 \psi \partial_x^2 \psi) + O(a^3) \quad (S4)$$

After simplifications and dropping total derivatives and constant energy contributions we obtain

$$S = \int_0^\beta d\tau a^{-1} \int_0^L dx i\psi \partial_\tau \theta + \frac{J}{2} a^2 \left( (\partial_x \psi)^2 + \frac{\psi^2 (\partial_x \psi)^2}{1 - \psi^2} + (1 - \psi^2) (\partial_x \theta)^2 \right) + g_1 \psi^2 + g_2 \psi^2 (\psi^2 + a^2 (\partial_x \psi)^2 + a^2 \psi \partial_x^2 \psi) \quad (S5)$$

Final expression for the Lagrangian with  $S = 1 = a$ , dropping linear terms in the fields and everything is to order  $O(a^2)$ :

$$\mathcal{L} = i\psi \partial_\tau \theta + \frac{J}{2} \left[ \frac{1}{1 - \psi^2} (\partial_x \psi)^2 + (1 - \psi^2) (\partial_x \theta)^2 \right] + g_1 \psi^2 + g_2 \psi^2 \left( \psi^2 + (\partial_x \psi)^2 + \psi \partial_x^2 \psi \right). \quad (S6)$$

last term  $\psi^3 \partial_x^2 \psi = -3\psi^2 (\partial_x \psi)^2$ , therefore, this to

$$\mathcal{L} = i\psi \partial_\tau \theta + \frac{J}{2} \left[ \frac{1}{1 - \psi^2} (\partial_x \psi)^2 + (1 - \psi^2) (\partial_x \theta)^2 \right] + g_1 \psi^2 + g_2 \psi^2 \left( \psi^2 - 2(\partial_x \psi)^2 \right). \quad (S7)$$

Integrating out the phase leads to

$$\mathcal{L} = \frac{1}{2J} \frac{\psi \partial_\tau^2 \nabla^{-2} \psi}{1 - \psi^2} + \frac{J}{2} \frac{(\partial_x \psi)^2}{1 - \psi^2} + g_1 \psi^2 + g_2 \psi^2 \left( \psi^2 - 2(\partial_x \psi)^2 \right). \quad (S8)$$

Following the argument of Landau-Ginzburg, we drop higher order  $\psi$ -terms since it is the order parameter and it becomes small at the second order phase transition  $\psi^2 \approx 0$

$$\mathcal{L} = \left[ \frac{1}{2J} \psi \partial_\tau^2 \nabla^{-2} \psi + \frac{J}{2} (\partial_x \psi)^2 \right] (1 + \psi^2) + g_1 \psi^2 + g_2 \psi^2 \left( \psi^2 - 2(\partial_x \psi)^2 \right) + O(\psi^6). \quad (S9)$$

Proposal for initial action

$$\mathcal{L} = \frac{1}{2} \partial_\tau^2 \nabla^{-2} \psi + \frac{1}{2} (\partial_x \psi)^2 + m \psi^2 + \lambda_0 \psi^4 + \lambda_1 \psi^3 \partial_\tau^2 \nabla^{-2} \psi + \lambda_2 \psi^2 (\partial_x \psi)^2. \quad (S10)$$

#### S4. Epsilon expansion

The bare massless Euclidean action (in imaginary time  $\tau$ ) is given by

$$S_0[\theta, \psi] = \int d^d x d\tau \left[ i \psi \partial_\tau \theta + \frac{K}{2} (\nabla \theta)^2 + \frac{1}{2} (\nabla \psi)^2 + \frac{g}{4!} \psi^4 \right]. \quad (S11)$$

With the Euclidean Fourier convention

$$f(\omega, p) = \int d^d x d\tau f(\tau, x) e^{-i\omega\tau - ipx}, \quad (S12)$$

the bare inverse propagator is given by

$$S^{(2)}(\omega, q) = \begin{pmatrix} q^2 & \omega \\ -\omega & K q^2 \end{pmatrix}, \quad (\text{S13})$$

with a field ordering  $(\psi, \theta)$ . The bare Green's function for the  $\psi$ -fields  $G_{0,\psi\psi}$ , we will denote as  $G_0(\omega, q) = \frac{K q^2}{\omega^2 + K q^4}$ . The poles are  $\omega_{1,2} = \pm i \sqrt{K} q^2$ . We note, that the bare propagator resembles the problem of the zero-temperature bosonic gas at vanishing fugacity.

### Multiplicative renormalization

We introduce in the following the renormalized action, depending on the renormalized coupling, indicated with an index  $R$ . We follow the derivation in Zinn-Justin's book [38] closely and for simplicity borrow their notation. The scale  $\mu$  is the renormalization scale, i.e. the symmetric momentum scale at which we evaluate the momenta of the 1PI correlation functions.

$$\theta = Z_\theta^{1/2} \theta_R, \quad \psi = Z_\psi^{1/2} \psi_R, \quad K = \frac{Z_K}{Z_\theta} K_R, \quad g = \frac{\mu^\varepsilon Z_g}{Z_\psi^2} g_R. \quad (\text{S14})$$

In MS with dimensional regularization only poles in  $\varepsilon$  are subtracted in the  $Z$ -factors.

$$S_R[\theta_R, \psi_R] = \int d^d x d\tau \left[ i (Z_\psi^{1/2} Z_\theta^{1/2}) \psi_R \partial_\tau \theta_R + \frac{1}{2} Z_K K_R (\nabla \theta_R)^2 + \frac{1}{2} Z_\psi (\nabla \psi_R)^2 + \frac{1}{4!} \mu^\varepsilon Z_g g_R \psi_R^4 \right]. \quad (\text{S15})$$

### Ward identities

The non-renormalizability of the Berry term leads to a Ward identity for the mixed two-point vertex at the normalization point:  $\partial_\omega \Gamma_R^{\psi\theta}|_{\text{NP}} = 1$ . This imposes the constraint among  $Z$ -factors:

$$Z_\psi^{1/2} Z_\theta^{1/2} = 1, \quad \Longleftrightarrow \quad Z_\psi = Z_\theta^{-1} \equiv Z. \quad (\text{S16})$$

Further, we note that the  $\theta$ -sector will get no corrections, as the theory is non-interacting. This can be seen, from the fact that no 1PI diagram with outer  $\theta$ -legs can be built. While  $G^{\theta\theta}$  is non-trivial due the interacting  $\psi$ -sector, the amputated two-point function  $\Gamma_R^{\theta\theta} = S^{\theta\theta}$  remains equal to the bare one. Hence, the renormalized coupling equals the bare one and we conclude that

$$Z_K K_R = K. \quad (\text{S17})$$

Note, that both Ward identities can be derived from  $\langle J_\theta \epsilon \rangle = \langle \delta S \rangle$  with the source field of the phase  $J_\theta = \Gamma^\theta$ , by noting that a infinitesimal space-time dependent shift of the phase

$$\theta(x, \tau) \mapsto \theta(x, t) + \epsilon(x, t), \quad (\text{S18})$$

varies the action to first order in the shift

$$\delta S = i\psi \partial_\tau \epsilon + K \nabla \theta \nabla \epsilon + \mathcal{O}(\epsilon^2). \quad (\text{S19})$$

### Ansatz

The effective action therefore reads

$$S_R[\theta_R, \psi_R] = \int d^d x d\tau \left[ i \psi_R \partial_\tau \theta_R + \frac{1}{2} K (\nabla \theta_R)^2 + \frac{1}{2} Z (\nabla \psi_R)^2 + \frac{1}{4!} \mu^\varepsilon Z_g g_R \psi_R^4 \right]. \quad (\text{S20})$$

This is astonishing as the number of running couplings corresponds exactly to the text book massless  $\phi^4$ -theory. From the Berry phase term can be seen that  $\psi$  and  $\theta$  are conjugate fields, moreover, their renormalization are locked together due to the first Ward identity.

### Massive theory

In order to introduce a mass to the theory, we add a source term for the monomial  $\psi_R^2$  to the action. We write

$$S_R[\theta_R, \psi_R, m_R] = S_R[\theta_R, \psi_R] + \frac{1}{2} m_R^2 \int_{x,\tau} Z_2 \psi_R^2, \quad (\text{S21})$$

where with respect to the initial action  $m^2 = m_R^2 Z_2 Z^{-1}$ .

### S5. One-loop correction

To one-loop order, we need to calculate only a single diagram that contributes at finite external momentum. This is the diagram  $B_d(\omega, q)$  that we evaluate and expand in  $\varepsilon$  about the upper critical dimension  $d_c = 2$  in Section S8.

### No correction to the field renormalization

First, we see that at one-loop order all  $Z$  factors of terms involving derivatives remain one. Here, the field renormalization

$$Z = 1 + \mathcal{O}(g_R^2). \quad (\text{S22})$$

### Four-point function

We calculate here the three channels of the diagram  $B_d(q)$ , see appendix and arrive to one-loop at

$$\tilde{\Gamma}_R^{(4)}(p_i) = g_R Z_g \mu^\varepsilon - \frac{1}{2} Z_g^2 g_R^2 \mu^{2\varepsilon} \left[ B_d(p_1 + p_2) + 2 \text{ channels} \right] + \mathcal{O}(g_R^3), \quad (\text{S23})$$

inserting the result at  $\mu = 1$ , we obtain in  $d = 2 - \varepsilon$  dimensions in the  $\overline{MS}$  scheme

$$\tilde{\Gamma}_R^{(4)}(p_i) = g_R Z_g - \frac{3}{2} Z_g^2 g_R^2 b_1 - \frac{1}{2} Z_g^2 g_R^2 \left[ B_r(p_1 + p_2) + 2 \text{ channels} \right] + \mathcal{O}(\varepsilon, g_R^3), \quad (\text{S24})$$

with  $B_{2-\varepsilon}^{(\overline{MS})}(q) = b_1 + B_r(q) + \mathcal{O}(\varepsilon)$ ,  $b_1 := \frac{\sqrt{K}}{4} N_2 \frac{1}{\varepsilon}$  being the divergent part in  $\varepsilon$ , but constant in momentum, and  $B_r(q) := -\frac{\sqrt{K}}{4} N_2 \left[ \frac{1}{2} \ln q^2 - \ln 2 \right]$  contains the IR divergence. Therefore,

$$Z_g = 1 + \frac{3}{2} \frac{\tilde{g}}{\varepsilon} + \mathcal{O}(\tilde{g}^2), \quad (\text{S25})$$

where we introduce an effective coupling, absorbing the loop factors

$$\tilde{g} := \frac{\sqrt{K}}{4} N_2 g_R. \quad (\text{S26})$$

### $\psi_R^2$ -insertion

We calculate the mixed three-point function

$$\tilde{\Gamma}_R^{(2,1)}(p_1, p_2) = Z_2 - \frac{1}{2} g_R Z_g Z_2 B_d(p_1 + p_2) + \mathcal{O}(g_R^2), \quad (\text{S27})$$

where the first index is a second order derivative with respect to the  $\psi_R$ -field and the second index the first derivative in the composite field  $\psi_R^2$ . We find at  $p_2 = 0$  to one-loop order

$$\tilde{\Gamma}_R^{(2,1)}(p, 0) = Z_2 - \frac{1}{2} g_R Z_g Z_2 (b_1 + B_r(p)) + \mathcal{O}(\varepsilon, g_R^2), \quad (\text{S28})$$

and find that

$$Z_2 = 1 + \frac{1}{2} \frac{\tilde{g}}{\varepsilon} + \mathcal{O}(\tilde{g}^2). \quad (\text{S29})$$

## S6. Two-loop order

To two-loop order, we need to calculate three different diagrams, conveniently called  $A$ ,  $B$  and  $C$ . To enhance the readability of the derivation, the evaluation of the frequency and momentum integrals, as well as the expansion about the upper critical dimension has been outsourced to Section S8.

### Two-point function

We start with the two-loop correction to the 1-PI self-energy of the renormalized two-point function in Fourier representation

$$\tilde{\Gamma}_R^{(2)}(q) = Z q^2 - \frac{1}{6} g_R^2 \mu^{2\varepsilon} A_d(q) + \mathcal{O}(g_R^3). \quad (\text{S30})$$

that gets a correction from the setting sun diagram  $A_d$ . With the result (S55) we can read off that the field renormalization becomes at  $\mu = 1$

$$Z = 1 - \frac{1}{54} \frac{1}{\varepsilon} \tilde{g}^2 + \mathcal{O}(\tilde{g}^3). \quad (\text{S31})$$

### Four-point function

To the next order we can obtain the correction to  $Z_g$  from the four-point function at two-loop order, comprised of

$$\begin{aligned} \tilde{\Gamma}_R^{(4)}(\omega_i, p_i) &= g_R Z_g \mu^\varepsilon - \frac{1}{2} g_R^2 Z_g^2 \mu^{2\varepsilon} [B_d(\omega_1 + \omega_2, p_1 + p_2) + 2 \text{ terms}] \\ &\quad + \frac{1}{4} g_R^3 \mu^{3\varepsilon} [B_d^2(\omega_1 + \omega_2, p_1 + p_2) + 2 \text{ terms}] \\ &\quad + \frac{1}{2} g_R^3 \mu^{3\varepsilon} [C_d(\omega_1, \omega_2, p_1, p_2) + 5 \text{ terms}] + \mathcal{O}(g_R^4). \end{aligned} \quad (\text{S32})$$

After setting  $\mu = 1$  and splitting  $B_d(p) = b_1 + B_r(p)$  as given in (S59), where  $B_r(p)$  is a constant in  $\varepsilon$ , the expansion becomes

$$\begin{aligned} \tilde{\Gamma}_R^{(4)}(p_i) &= g_R Z_g - \frac{3}{2} b_1 g_R^2 Z_g^2 - \frac{1}{2} Z_g^2 g_R^2 [B_r(p_1 + p_2) + 2 \text{ terms}] \\ &\quad + \frac{1}{4} g_R^3 [B_r^2(p_1 + p_2) + 2 \text{ terms}] + \frac{1}{2} b_1 g_R^3 [B_r(p_1 + p_2) + 2 \text{ terms}] + \frac{3}{4} b_1^2 g_R^3 \\ &\quad + \frac{1}{2} g_R^3 [C_d(p_1, p_2) + 5 \text{ terms}]. \end{aligned} \quad (\text{S33})$$

We use the result of  $Z_g$  to one-loop order (S22) to simplify perturbative expansion and extract the  $Z_g$  to next order

$$\begin{aligned} \tilde{\Gamma}_R^{(4)}(p_i) &= g_R Z_g - \frac{3}{2} b_1 g_R^2 - \frac{15}{4} b_1^2 g_R^3 - \frac{1}{2} g_R^2 [B_r(p_1 + p_2) + 2 \text{ terms}] \\ &\quad + \frac{1}{4} g_R^3 [B_r^2(p_1 + p_2) + 2 \text{ terms}] + \frac{1}{2} g_R^3 [C(p_1, p_2) - b_1 B_r(p_1 + p_2) + 5 \text{ terms}]. \end{aligned} \quad (\text{S34})$$

Now, we make use of the fact that the IR-divergence in diagram  $C_d$  comes from the subdiagram  $B_d$ , which cancels exactly. The divergent part of the combination of the diagrams  $[C_d(p_1, p_2) - b_1 B_r(p_1 + p_2)]_{2-\varepsilon}$  is therefore momentum-independent and given by

$$\begin{aligned} D_{\text{div}} &= C_{2-\varepsilon}^{(\overline{MS})}(q) - b_1 B_r(q) \\ &= \frac{K N_2^2}{16} \left\{ \frac{1}{8} \left[ \frac{4}{\varepsilon^2} + \left( \frac{1}{3} + 12 \ln 2 - 2 \ln 3 - 4 \ln q^2 \right) \frac{1}{\varepsilon} \right] + \frac{1}{\varepsilon} \left[ \frac{1}{2} \ln q^2 - \ln 2 \right] + \mathcal{O}(\varepsilon^0) \right\} \\ &= \frac{K N_2^2}{16} \frac{1}{8} \left[ \frac{4}{\varepsilon^2} + \left( \frac{1}{3} + 4 \ln 2 - 2 \ln 3 \right) \frac{1}{\varepsilon} \right] + \mathcal{O}(\varepsilon^0). \end{aligned} \quad (\text{S35})$$

Hence, the divergent part of  $\Gamma^{(4)}$  reduces to

$$[\tilde{\Gamma}_R^{(4)}(p_i)]_{\text{div}} = g_R Z_g - \frac{3}{2} b_1 g_R^2 - \frac{15}{4} b_1^2 g_R^3 + 3 g_R^3 D_{\text{div}}. \quad (\text{S36})$$

We can read off

$$Z_g = 1 + \frac{3}{2} b_1 g_R + \frac{15}{4} b_1^2 g_R^2 - 3g_R^2 D_{\text{div}} \quad (\text{S37})$$

$$= 1 + \frac{3}{2} \frac{\tilde{g}}{\varepsilon} + \tilde{g}^2 \left[ \frac{9}{4} \frac{1}{\varepsilon^2} + \frac{1}{\varepsilon} \left( \frac{1}{8} + \frac{3}{2} \ln 2 - \frac{3}{4} \ln 3 \right) \right] + \mathcal{O}(\tilde{g}^3, \varepsilon^0). \quad (\text{S38})$$

### $\psi_R^2$ -insertion

We can calculate the correction to the mass from the three-point function at two-loop order

$$\begin{aligned} \tilde{\Gamma}_R^{(2,1)}(\omega_1, \omega_2, p_1, p_2) &= Z_2 - \frac{1}{2} g_R Z_g Z_2 B_d(\omega_1 + \omega_2, p_1 + p_2) + \frac{1}{4} g_R^2 B_d^2(\omega_1 + \omega_2, p_1 + p_2) \\ &\quad + \frac{1}{2} g_R^2 C_d(\omega_1, \omega_2, p_1, p_2) + \mathcal{O}(g_R^3). \end{aligned} \quad (\text{S39})$$

Analogous to the previous section, we split  $B_d$  and  $C_d$ , given in (S59) and (S90) respectively, again into momentum independent, divergent terms and momentum-dependent ones, insert the result for  $Z_g$  and then  $Z_2$  at one loop order and find the divergent part of the three-point function to be given by

$$[\tilde{\Gamma}_R^{(2,1)}(p, 0)]_{\text{div.}} = Z_2 - \frac{1}{2} b_1 g_R - \frac{3}{4} b_1^2 g_R^2 + \frac{1}{2} g_R^2 D_{\text{div}} + \mathcal{O}(g_R^3). \quad (\text{S40})$$

Requiring that this amputated Green's function vanishes at two-loop order leaves us with

$$Z_2 = 1 + \frac{1}{2} \frac{\tilde{g}}{\varepsilon} + \tilde{g}^2 \left[ \frac{1}{2} \frac{1}{\varepsilon^2} - \frac{1}{16} \left( \frac{1}{3} + 4 \ln 2 - 2 \ln 3 \right) \frac{1}{\varepsilon} \right] + \mathcal{O}(\tilde{g}^3, \varepsilon^0). \quad (\text{S41})$$

## S7. Critical exponents

The dimension of the renormalized field is given by  $[\psi_R]_\mu = \Delta_\psi = \frac{1}{2}(D - 2 + \eta)$  with  $D = d + z$ . The anomalous exponent is defined as the scaling of  $Z$  at the fixed point

$$\eta \equiv \eta(\tilde{g}^*) := \mu \partial_\mu \ln Z|_*, \quad (\text{S42})$$

where  $\mu \partial_\mu \ln Z = \beta(g_R) \frac{d}{dg_R} \ln Z(g_R)$ , with  $\beta(g_R) \equiv \mu \partial_\mu g_R = -\varepsilon \left( \frac{d \ln G(g_R)}{dg_R} \right)^{-1}$  and  $G(g_R) = \frac{g_R Z_g}{Z^2}$ . Further, we define  $\eta_2(g_R) := \beta(g_R) \frac{d}{dg_R} \ln \frac{Z_2(g_R)}{Z(g_R)}$ , which gives the critical exponent  $\nu = (\eta_2(g_R^*) + 2)^{-1}$ .

Integrating out the  $\theta$  phase, we find the renormalized action

$$\tilde{S}_R[\psi_R] = \int d^d x d\tau \left[ \frac{1}{2K} \psi_R \partial_\tau^2 \nabla^{-2} \psi_R + \frac{1}{2} Z (\nabla \psi_R)^2 + \frac{1}{4!} \mu^\varepsilon Z_g g_R \psi_R^4 \right]. \quad (\text{S43})$$

From the first term of the action, which does not renormalize, we get a relation for the renormalized field dimension  $2\Delta_\psi = d - z + 2$ , which implies that the dynamical critical exponent  $z$  is given by  $\eta$

$$z = 2 - \frac{\eta}{2}. \quad (\text{S44})$$

### To first order

We find from the first order result that the  $\beta$ -function is given by

$$\tilde{\beta}(\tilde{g}) := \frac{\tilde{g}}{g_R} \beta(\tilde{g}) = -\varepsilon \tilde{g} + \frac{3}{2} \tilde{g}^2 + \mathcal{O}(\tilde{g}^3), \quad (\text{S45})$$

equivalent to the Ising one and find the non-trivial fixed point at  $\tilde{g}^* = \frac{2}{3}\varepsilon$ .

### To second order

We get

$$\tilde{\beta}(\tilde{g}) = -\varepsilon\tilde{g} + \frac{3}{2}\tilde{g}^2 + \gamma_1\tilde{g}^3 + \mathcal{O}(\tilde{g}^4) \quad \text{with} \quad \gamma_1 := \frac{2}{27} + \frac{1}{4} + 3\ln 2 - \frac{3}{2}\ln 3, \quad (\text{S46})$$

$$\eta(\tilde{g}) = \frac{1}{27}\tilde{g}^2 + \mathcal{O}(\tilde{g}^3), \quad (\text{S47})$$

$$\eta_2(\tilde{g}) = -\frac{\tilde{g}}{2} + \gamma_2\tilde{g}^2 + \mathcal{O}(\tilde{g}^3), \quad \text{with} \quad \gamma_2 := -\frac{1}{2}\ln 2 + \frac{1}{4}\ln 3 - \frac{1}{24} - \frac{1}{27}, \quad (\text{S48})$$

which is different from correction in the Ising model. The positive, non-zero fixed point solution is given to second order in epsilon by  $\tilde{g}^* = \frac{2}{3}\varepsilon - \frac{8}{27}\gamma_1\varepsilon^2 + \mathcal{O}(\varepsilon^3)$ .

We obtain  $\eta = \frac{4}{243}\varepsilon^2$ , hence  $z = 2 - \frac{2}{243}\varepsilon^2$  and  $2\nu = 1 + \frac{1}{6}\varepsilon - [\frac{1}{36} + \frac{2}{9}\gamma_2 + \frac{2}{27}\gamma_1]\varepsilon^2 + \mathcal{O}(\varepsilon^3)$ , with  $[\frac{1}{36} + \frac{2}{9}\gamma_2 + \frac{2}{27}\gamma_1] \approx 0.050$ .

### S8. Evaluation of loop integrals and expansion about $d_c = 2$

We introduce the loop factor

$$N_d = \frac{2}{(4\pi)^{d/2}} \frac{1}{\Gamma(\frac{d}{2})}, \quad \int \frac{d^d p}{(2\pi)^d} = N_d \int_0^\infty dp p^{d-1}, \quad (\text{S49})$$

with  $N_2 = 1/(2\pi)$  in two dimensions. Further, the bare propagator is given by  $G_0(\omega_q, q) = \frac{Kq^2}{\omega_q^2 + Kq^4}$  and we define  $F_q = \sqrt{K}q^2$ .

### Two-point function

The setting sun diagram is given by

$$A_d(\omega_q, q) \equiv \int \frac{d\omega_k}{2\pi} \frac{d^d k}{(2\pi)^d} \int \frac{d\omega_p}{2\pi} \frac{d^d p}{(2\pi)^d} G_0(\omega_k, k) G_0(\omega_p, p) G_0(\omega_q - \omega_k - \omega_p, q - k - p). \quad (\text{S50})$$

Using the convolution identity (for  $F_1, F_2 \in \mathbb{R}^+$ )

$$\int_{-\infty}^{\infty} \frac{d\omega}{2\pi} \frac{1}{(\omega^2 + F_1^2)[(\omega_x - \omega)^2 + F_2^2]} = \frac{F_1 + F_2}{2F_1 F_2 (\omega_x^2 + (F_1 + F_2)^2)}, \quad (\text{S51})$$

first with  $F_1 = F_p, F_2 = F_{q-p-k}, \omega_x = \omega_q - \omega_k$ , and then over  $\omega_k$  with  $F_1 = F_k, F_2 = F_p + F_{q-p-k}, \omega_x = \omega_q$ , we obtain

$$A_d(\omega_q, q) = \frac{K^{3/2}}{4} \int \frac{d^d p}{(2\pi)^d} \frac{d^d k}{(2\pi)^d} \frac{\mathcal{F}(q, p, k)}{\omega_q^2 + \mathcal{F}(q, p, k)^2}, \quad \mathcal{F}(q, p, k) := F_p + F_k + F_{q-p-k}. \quad (\text{S52})$$

In the static limit  $\omega_q = 0$ , we can evaluate the double momentum integral to

$$A_d(0, q) = \frac{K}{4} \int \frac{d^d p}{(2\pi)^d} \frac{d^d k}{(2\pi)^d} \frac{1}{(q - p - k)^2 + p^2 + k^2} = \frac{K}{16} 3^{1-\frac{3d}{2}} N_d^2 \Gamma(1-d) \Gamma\left(\frac{d}{2}\right)^2 (q^2)^{d-1}. \quad (\text{S53})$$

Now, in order to obtain the field renormalization, we calculate

$$\partial_{q^2} A_d(0, q) = -\frac{K}{16} 3^{1-\frac{3d}{2}} N_d^2 \Gamma(2-d) \Gamma\left(\frac{d}{2}\right)^2 (q^2)^{d-2} \quad (\text{S54})$$

which returns in  $d = 2 - \varepsilon$  in  $\overline{MS}$  scheme (see below)

$$\partial_{q^2} A_{2-\varepsilon}^{(\overline{MS})}(0, q) = -\frac{K N_2^2}{144} \frac{1}{\varepsilon} \left[ 1 + \varepsilon \left( \frac{3}{2} \ln 3 - \ln(q^2) \right) \right] + \mathcal{O}(\varepsilon). \quad (\text{S55})$$

### Four-point function - first diagram

The one-loop diagram correction to the four-point interaction reads

$$B(\omega_q, q) \equiv \int \frac{d\omega_p}{2\pi} \frac{d^d p}{(2\pi)^d} G_0(\omega_p, p) G_0(\omega_p + \omega_q, p + q) = \frac{K}{2} \int_p \frac{F_p + F_{p+q}}{\omega_q^2 + (F_p + F_{p+q})^2}. \quad (\text{S56})$$

For  $\omega_q = 0$ , we find

$$B_d(0, q) = \frac{\sqrt{K}}{2^{d+1}} N_d \Gamma\left(\frac{d}{2}\right) \Gamma\left(1 - \frac{d}{2}\right) (q^2)^{d/2-1}. \quad (\text{S57})$$

Now, we apply the  $\overline{MS}$ -scheme, i.e., multiply the result by  $N_2/N_d$ . Hence, in  $d = 2 - \varepsilon$  dimensions, the Laurent series reads to leading order

$$B_{2-\varepsilon}^{\overline{MS}}(q) = b_1 + B_r(q) + \mathcal{O}(\varepsilon), \quad (\text{S58})$$

where we separated  $b_1$  the divergent part in  $\varepsilon$ , from the momentum dependent (IR divergent) part  $B_r(q)$

$$b_1 = \frac{\sqrt{K}}{4} N_2 \frac{1}{\varepsilon}, \quad B_r(q) = -\frac{\sqrt{K}}{4} N_2 \left[ \frac{1}{2} \ln q^2 - \ln 2 \right]. \quad (\text{S59})$$

### Four-point function - second diagram

The last two-loop diagram we need is given by

$$\tilde{C}_d(\omega_{q_1}, q_1, 0, 0) \equiv \int \frac{d\omega_k}{2\pi} \frac{d^d k}{(2\pi)^d} \int \frac{d\omega_p}{2\pi} \frac{d^d p}{(2\pi)^d} G_0(\omega_p + \omega_{q_1}, p + q_1) G_0(\omega_p, p) G_0(\omega_p - \omega_k, p - k) G_0(\omega_k, k). \quad (\text{S60})$$

We integrate out  $\omega_k$  making use of the convolution (S51), then using

$$\begin{aligned} & \int_{-\infty}^{\infty} \frac{d\omega_p}{2\pi} \frac{1}{(\omega_p^2 + F_p^2) [(\omega_p + \omega_q)^2 + F_{p+q}^2] (\omega_p^2 + F_x^2)} \\ &= \frac{1}{2(F_x^2 - F_p^2)} \left[ \frac{1}{F_p((\omega_q + iF_p)^2 + F_{p+q}^2)} - \frac{1}{F_x((\omega_q + iF_x)^2 + F_{p+q}^2)} \right] \\ &+ \frac{1}{2F_{p+q}((- \omega_q + iF_{p+q})^2 + F_p^2) ((- \omega_q + iF_{p+q})^2 + F_x^2)}, \end{aligned} \quad (\text{S61})$$

with additionally  $\omega_{q_1} = 0$  and  $C_d(q) = \tilde{C}_d(0, q, 0, 0)$ , we find the expression in terms of momentum integrals to be

$$C_d(q) = \frac{K^2}{4} \int_{p,k} \frac{F_p + F_{p+q} + F_{p-k} + F_k}{(F_p + F_{p+q})(F_{p+q} + F_{p-k} + F_k)(F_p + F_{p-k} + F_k)} \quad (\text{S62})$$

$$= \frac{K}{4} \int \frac{d^d p}{(2\pi)^d} \frac{d^d k}{(2\pi)^d} \frac{p^2 + (p+q)^2 + (p-k)^2 + k^2}{[p^2 + (p+q)^2] [(p+q)^2 + (p-k)^2 + k^2] [p^2 + (p-k)^2 + k^2]}. \quad (\text{S63})$$

Introduce

$$D_{12} := p^2 + (p+q)^2, \quad D_{23} := (p+q)^2 + (p-k)^2 + k^2, \quad D_{13} := p^2 + (p-k)^2 + k^2,$$

such that the integrand splits as

$$\frac{p^2 + (p+q)^2 + (p-k)^2 + k^2}{D_{12} D_{13} D_{23}} = \frac{1}{2} \left( \frac{1}{D_{13} D_{23}} + \frac{1}{D_{12} D_{23}} + \frac{1}{D_{12} D_{13}} \right). \quad (\text{S64})$$

With a Feynman parameter, we can solve the  $p$  integration and obtain

$$C_d(q) = \frac{K}{2^5 (4\pi)^{d/2}} \Gamma\left(2 - \frac{d}{2}\right) \int \frac{d^d k}{(2\pi)^d} \sum_{ij \in \{12, 13, 23\}} \int_0^1 dx (\tilde{S}_{ij}(x))^{\alpha_p}, \quad \alpha_p := \frac{d}{2} - 2, \quad (\text{S65})$$

with the shorthand

$$\tilde{S}_{ij}(x) = A_{ij}(x) Q^2 + B_{ij}(x) r^2 + C_{ij}(x) Q r \mu, \quad Q := |\mathbf{q}|, \quad r := |\mathbf{k}|, \quad \mu := \frac{\mathbf{q} \cdot \mathbf{k}}{Q r}, \quad (\text{S66})$$

and the channel polynomials

$$\begin{aligned} (12) : A_{12} &= (1 - x^2)/4, & B_{12} &= 3/4, & C_{12} &= (1 - x)/2, \\ (13) : A_{13} &= 1/4, & B_{13} &= (3 - 2x - x^2)/4, & C_{13} &= (1 - x)/2, \\ (23) : A_{23} &= x(2 - x)/4, & B_{23} &= (3 - 2x - x^2)/4, & C_{23} &= x(1 - x)/2. \end{aligned} \quad (\text{S67})$$

#### Angular and radial $k$ -integrations

For  $\text{Re } a > 0$ ,

$$\int d\Omega_{d-1} (a + b\mu)^\alpha = \frac{2\pi^{d/2}}{\Gamma(d/2)} a^\alpha {}_2F_1\left(-\alpha, \frac{1}{2}; \frac{d}{2}; \frac{b^2}{a^2}\right), \quad (\text{S68})$$

with  $a = A_{ij}Q^2 + B_{ij}r^2$ ,  $b = C_{ij}Qr$  and using the hypergeometric function  ${}_2F_1$ . Hence

$$\begin{aligned} C_d(q) &= \frac{K \Gamma(2 - \frac{d}{2})}{2^5 (4\pi)^{d/2}} \frac{2\pi^{d/2}}{\Gamma(d/2)} \frac{1}{(2\pi)^d} \sum_{ij} \int_0^1 dx \int_0^\infty dr r^{d-1} (A_{ij}Q^2 + B_{ij}r^2)^{\alpha_p} \\ &\quad \times {}_2F_1\left(-\alpha_p, \frac{1}{2}; \frac{d}{2}; \frac{C_{ij}^2 Q^2 r^2}{(A_{ij}Q^2 + B_{ij}r^2)^2}\right). \end{aligned} \quad (\text{S69})$$

Let  $t = r^2$  ( $r^{d-1} dr = \frac{1}{2} t^{\frac{d}{2}-1} dt$ ) and map

$$y = \frac{B_{ij}t}{A_{ij}Q^2 + B_{ij}t} \in (0, 1), \quad \frac{C_{ij}^2 Q^2 t}{(A_{ij}Q^2 + B_{ij}t)^2} = \frac{C_{ij}^2}{A_{ij}B_{ij}} y(1 - y). \quad (\text{S70})$$

together with  $\frac{dy}{y(1-y)} = \frac{dt}{t}$ . After simplifying constants one finds

$$C_d(q) = \frac{K \Gamma(2 - \frac{d}{2})}{2^{2d+5} \pi^d \Gamma(\frac{d}{2})} Q^{2(d-2)} \sum_{ij} \int_0^1 dx A_{ij}^{d-2} B_{ij}^{-d/2} I_y(\lambda_{ij}(x)), \quad (\text{S71})$$

where, for clarity of notation,  $\alpha = \frac{d}{2}$ ,  $\beta = 2 - \frac{d}{2}$  and

$$I_y(\lambda) = \int_0^1 y^{\alpha-1} (1-y)^{\beta-\alpha-1} {}_2F_1\left(\beta, \frac{1}{2}; \alpha; \lambda y(1-y)\right) dy, \quad \lambda_{ij} = \frac{C_{ij}^2}{A_{ij}B_{ij}}. \quad (\text{S72})$$

#### Formulas used

In the following two sections, we make extensive use of the integral representations and series expansions in terms of Pochhammer symbols of the hypergeometric function  ${}_2F_1$ , a generalized hypergeometric function, the Appel series, (incomplete) Beta-functions. We provide the necessary expressions, consult for instance [47].

Definition of the Appell  $F_1$

$$F_1(a; b_1, b_2; c; x, y) = \frac{\Gamma(c)}{\Gamma(a)\Gamma(c-a)} \int_0^1 u^{a-1} (1-u)^{c-a-1} (1-xu)^{-b_1} (1-yu)^{-b_2} du, \quad (\text{S73})$$

valid for  $\text{Re}(c) > \text{Re}(a) > 0$ . The series expansion is

$$F_1(a; b_1, b_2; c; x, y) = \sum_{m=0}^{\infty} \sum_{n=0}^{\infty} \frac{(a)_{m+n} (b_1)_m (b_2)_n}{(c)_{m+n}} \frac{x^m}{m!} \frac{y^n}{n!}, \quad (|x| < 1, |y| < 1), \quad (\text{S74})$$

given in terms of the rising Pochhammer symbols

$$(q)_0 = 1, \quad (q)_n = q(q+1) \cdots (q+n-1) = \frac{\Gamma(q+n)}{\Gamma(q)}. \quad (\text{S75})$$

The incomplete Beta-function is given by

$$B_z(a, b) = \int_0^z t^{a-1} (1-t)^{b-1} dt = \frac{z^a}{a} {}_2F_1(a, 1-b; a+1; z). \quad (\text{S76})$$

And for  $z = 1$ , the Beta-function, can be given in terms of Gamma-functions

$$B(a, b) = \int_0^1 t^{a-1} (1-t)^{b-1} dt = \frac{\Gamma(a) \Gamma(b)}{\Gamma(a+b)}. \quad (\text{S77})$$

*y-integration (closed form)*

Expanding the Gauss function and integrating termwise, we obtain

$$\int_0^1 y^{\alpha-1+n} (1-y)^{\beta-\alpha-1+n} dy = B(\alpha+n, \beta-\alpha+n) = \frac{\Gamma(\alpha) \Gamma(\beta-\alpha)}{\Gamma(\beta)} \frac{(\alpha)_n (\beta-\alpha)_n}{(\beta)_{2n}}. \quad (\text{S78})$$

Using  $(\beta)_{2n} = 2^{2n} (\frac{\beta}{2})_n (\frac{\beta+1}{2})_n$ , we write the result in terms of a generalized hypergeometric function

$$\sum_{n=0}^{\infty} \frac{(\beta)_n (\frac{1}{2})_n}{(\alpha)_n n!} B(\alpha+n, \beta-\alpha+n) \lambda^n = \frac{\Gamma(\alpha) \Gamma(\beta-\alpha)}{\Gamma(\beta)} {}_3F_2\left(\beta, \beta-\alpha, \frac{1}{2}; \frac{\beta}{2}, \frac{\beta+1}{2}; \frac{\lambda}{4}\right). \quad (\text{S79})$$

Inserting into (S71) and canceling  $\Gamma(\frac{d}{2})$  gives the prefactor

$$C_d(q) = \frac{K \Gamma(2-d)}{2^{2d+5} \pi^d} Q^{2(d-2)} \sum_{ij} \int_0^1 dx A_{ij}^{d-2} B_{ij}^{-d/2} {}_3F_2\left(2-\frac{d}{2}, 2-d, \frac{1}{2}; 1-\frac{d}{4}, \frac{3}{2}-\frac{d}{4}; \frac{\lambda_{ij}(x)}{4}\right). \quad (\text{S80})$$

*Series expansion and x-integration: final double sum*

Using

$$A_{ij}^{d-2} B_{ij}^{-d/2} \left(\frac{\lambda_{ij}}{4}\right)^n = \frac{C_{ij}^{2n}}{4^n} A_{ij}^{d-2-n} B_{ij}^{-d/2-n}, \quad (\text{S81})$$

define the channel moments

$$\mathcal{I}_n^{(ij)} := \int_0^1 dx C_{ij}(x)^{2n} A_{ij}(x)^{d-2-n} B_{ij}(x)^{-d/2-n}. \quad (\text{S82})$$

Then (S80) becomes the explicit double sum

$$C_d(q) = \frac{K \Gamma(2-d)}{2^{2d+5} \pi^d} Q^{2(d-2)} \sum_{n=0}^{\infty} \frac{(2-\frac{d}{2})_n (2-d)_n (\frac{1}{2})_n}{(1-\frac{d}{4})_n (\frac{3}{2}-\frac{d}{4})_n n! 4^n} \sum_{ij \in \{12, 13, 23\}} \mathcal{I}_n^{(ij)}. \quad (\text{S83})$$

we can evaluate the different channels by means of substitutions, which we give for each function and representations of corresponding hypergeometric functions. For the first channel, we substituted with  $x = 1 - 2u$ , to arrive at

$$\mathcal{I}_n^{(12)} = \frac{2^n 3^{-\frac{d}{2}-n}}{d-1+n} {}_2F_1\left(d-1+n, 2-d+n; d+n; \frac{1}{2}\right), \quad (\text{S84})$$

in the second, again with  $x = 1 - 2u$ , then  $u = 2v$ , to obtain

$$\mathcal{I}_n^{(13)} = \frac{2^{-2d+4}}{n+1-\frac{d}{2}} {}_2F_1\left(n+1-\frac{d}{2}, n+\frac{d}{2}; n+2-\frac{d}{2}; \frac{1}{4}\right), \quad (\text{S85})$$

and finally, in the third, no simplification could be found, such that we arrive at

$$\mathcal{I}_n^{(23)} = 2^{n+2} 3^{-\frac{d}{2}-n} \frac{\Gamma(n+d-1) \Gamma(n+1-\frac{d}{2})}{\Gamma(2n+\frac{d}{2})} F_1\left(n+d-1; n+2-d, \frac{d}{2}+n; 2n+\frac{d}{2}; \frac{1}{2}, -\frac{1}{3}\right). \quad (\text{S86})$$

with  $F_1$  being the Appell  $F_1$  function, compare Equation (S73).

#### Expansion in $\overline{MS}$ scheme

As before, we multiply with  $(N_2/N_d)^2$  and obtain

$$C_d^{(\overline{MS})}(q) = \frac{K N_2^2 \Gamma(2-d) \Gamma(\frac{d}{2})^2}{2^7} Q^{2(d-2)} \sum_{n=0}^{\infty} \frac{(2-\frac{d}{2})_n (2-d)_n (\frac{1}{2})_n}{(1-\frac{d}{4})_n (\frac{3}{2}-\frac{d}{4})_n n! 4^n} \sum_{ij \in \{12, 13, 23\}} \mathcal{I}_n^{(ij)}. \quad (\text{S87})$$

In order to expand the expression (S87), we represented the channels in terms of (double) sums and expanded them to the necessary order in  $\varepsilon$ , we will find that

$$\mathcal{I}_0^{(12)} = \frac{1}{3} + \mathcal{O}(\varepsilon), \quad (\text{S88})$$

$$\mathcal{I}_0^{(13)} = \frac{2}{\varepsilon} + 6 \ln 2 - \ln 3 + \mathcal{O}(\varepsilon) = \mathcal{I}_0^{(23)},$$

$$\mathcal{I}_n^{(ij)} = \mathcal{O}(\varepsilon^0), \quad \forall n > 0, ij \in \{12, 13, 23\}. \quad (\text{S89})$$

We used several times Equation (S92), and arrive at

$$C_{2-\varepsilon}^{(\overline{MS})}(q) = \frac{K N_2^2}{2^7} \left[ \frac{4}{\varepsilon^2} + \left( \frac{1}{3} + 12 \ln 2 - 2 \ln 3 - 4 \ln q^2 \right) \frac{1}{\varepsilon} + \mathcal{O}(\varepsilon^0) \right]. \quad (\text{S90})$$

#### Used trick on expansion for the hypergeometric functions

Let  $a = \mathcal{O}(\varepsilon)$ , and  $b = b_0 + \mathcal{O}(\varepsilon) = c$ , where  $b_0$  is a non-zero constant and  $|z| < 1$ , we want to show that the hypergeometric series,

$${}_2F_1(a, b; c; z) = \sum_{n=0}^{\infty} \frac{(a)_n (b)_n}{(c)_n} \frac{z^n}{n!}, \quad (\text{S91})$$

gives

$${}_2F_1(a, b; c; z) = 1 - a \ln(1-z) + \mathcal{O}(\varepsilon^2). \quad (\text{S92})$$

to linear order in  $\varepsilon$ .

Note, for  $n = 0$  the term is 1 and has no  $\varepsilon$ -dependence. For every  $n \geq 1$ ,  $(a)_n$  is  $\mathcal{O}(a) = \mathcal{O}(\varepsilon)$ , while the deviations of  $b$  and  $c$  from  $b_0$  are also  $\mathcal{O}(\varepsilon)$ . Thus any correction from  $b$  or  $c$  would multiply  $a$  and be  $\mathcal{O}(\varepsilon^2)$ , which we can drop at linear order.

Therefore, to  $\mathcal{O}(\varepsilon)$  we may set  $b = c = b_0$  in the  $n \geq 1$  terms. Further, for small  $a$ , one has  $(a)_n = a(a+1) \cdots (a+n-1) = a(n-1)! + \mathcal{O}(a^2)$ . Hence

$$\sum_{n=1}^{\infty} \frac{(a)_n}{n!} z^n = a \sum_{n=1}^{\infty} \frac{z^n}{n} + \mathcal{O}(a^2) = a(-\ln(1-z)) + \mathcal{O}(a^2), \quad (\text{S93})$$

and therefore the claim is shown.